Optimal Control of Walking with Functional Electrical Stimulation: A Computer Simulation Study

Dejan Popović, Richard B. Stein, M. Namik Oğuztöreli, Maria Lebiedowska, and Slavica Jonić, *Student Member, IEEE*

***Abstract*— Bipedal locomotion was simulated to generate a pattern of activating muscles for walking using electrical stimulation in persons with spinal cord injury (SCI) or stroke. The simulation presented in this study starts from a model of the body determined with user-specific parameters, individualized with respect to the lengths, masses, inertia, muscle and joint properties. The trajectory used for simulation was recorded from an able-bodied subject while walking with ankle-foot orthoses. A discrete mathematical model and dynamic programming were used to determine the optimal control. A cost function was selected as the sum of the squares of the tracking errors from the desired trajectories, and the weighted sum of the squares of agonist and antagonist activations of the muscle groups acting around the hip and knee joints. The aim of the simulation was to study plausible trajectories keeping in mind the limitations imposed by the spinal cord injury or stroke (e.g., spasticity, decreased range of movements in some joints, limited strength of paralyzed, externally activated muscles). If the muscles were capable of generating the movements required and the trajectory was achieved, then the simulation provided two kinds of information: 1) timing of the onset and offset of muscle activations with respect to the various gait events and 2) patterns of activation with respect to the maximum activation. These results are important for synthesizing a rule-based controller.**

***Index Terms*—Dynamic programming, optimal tracking, paraplegia, walking.**

I. Introduction

MULTIMCHANNEL functional electrical stimulation (FES) systems with surface electrodes [32], or percutaneous electrodes [5], [30] are in limited use for gait restoration. One of the constraints for wider usage of FES systems is the lack of efficient control. In FES systems, in home or clinical applications, a set of switches must be controlled volitionally for up to six channels of stimulation [32], or a preprogrammed sequence of stimulation patterns is applied to as many as 48 muscles [30]. Tuning the stimulation patterns is “hand-crafted” for each user [30]. Several more sophisticated control strategies are presented in the literature, involving open-loop [7], [8], [30], [38], [46], [51], [56], closed-loop [8], [14], [27], [28], [34] or nonanalytical control [1], [2], [13], [22], [29], [44], [49], [50], but none is yet sufficiently practical to be widely used.

The lower extremities of a walking human can be represented as a complex, multiactuator, redundant, mechanical system. Many methods have been employed to simulate the movements of human limbs [3], [12], [25]–[28], [31], [35], [39], [40], [48], but the biomechanical models [17], [18], [58] are generally very difficult to customize for a given individual, due to their complexity and poor user interface. Hatze [18], [21] used the traditional Lagrangian approach to derive a mathematical model of the total human musculoskeletal system. The model contained a linked set of ordinary first-order differential equations that describe the dynamics of the segments and muscles respectively. With this model Hatze [18] simulated the model with 17 segments and 46 muscles.

Zajac *et al.* [27], [28], [56], [58] developed a planar computer model to investigate paraplegic standing induced by FES. Yamaguchi and Zajac [56] tried to determine the minimal set of muscles that could approximate able-bodied gait trajectories without requiring either higher levels of force or precise control of muscle activation. They suggested that gait was more sensitive to changes in the on/off timing of the muscle stimulus than to its amplitude. The process of adjusting the muscle activation levels was critically dependent upon accurately understanding the effect of each muscle on the dynamic response of the system.

A systematic approach to include detailed biomechanical models for control of FES systems (e.g., [10], [13], [19], [20], [56], [58]) has advantages for analyzing the performance of a multichannel FES system. The models used are generally simplified by limiting the number of degrees of freedom; joints are reduced to simple machine-like structures and body segments are treated as rigid bodies. In theory, with appropriate data and constraints a model can predict the resultant actions between linkages to produce the motion [6], although there is considerable redundancy in the mechanical system [11], [16], [41].

One approach to dealing with the problem of redundancy has been to use optimization methods in which the equivalent

Manuscript received July 3, 1996; revised December 20, 1996, May 30, 1997, and August 24, 1998. This work was supported in part by the Medical Research Council of Canada, the Natural Sciences and Engineering Research Council of Canada, and the Ministry for Science and Technology of Serbia, Belgrade, Yugoslavia.

D. Popović and S. Jonić are with the Faculty of Electrical Engineering, University of Belgrade, Belgrade, Yugoslavia.

R. B. Stein is with the Division of Neuroscience, University of Alberta, Edmonton, Alta. T6G 2S2 Canada.

M. N. Oğuztöreli is with the Department of Mathematics, University of Alberta, Edmonton, Alta. T6G 2S2 Canada.

M. Lebiedowska was with the Division of Neuroscience, University of Alberta, Edmonton, Alta. T6G 2S2 Canada. She is now with the Division of Orthopedics and Rehabilitation, Southern Illinois University, Springfield, IL 62901 USA.

Publisher Item Identifier S 1063-6528(99)01168-4.

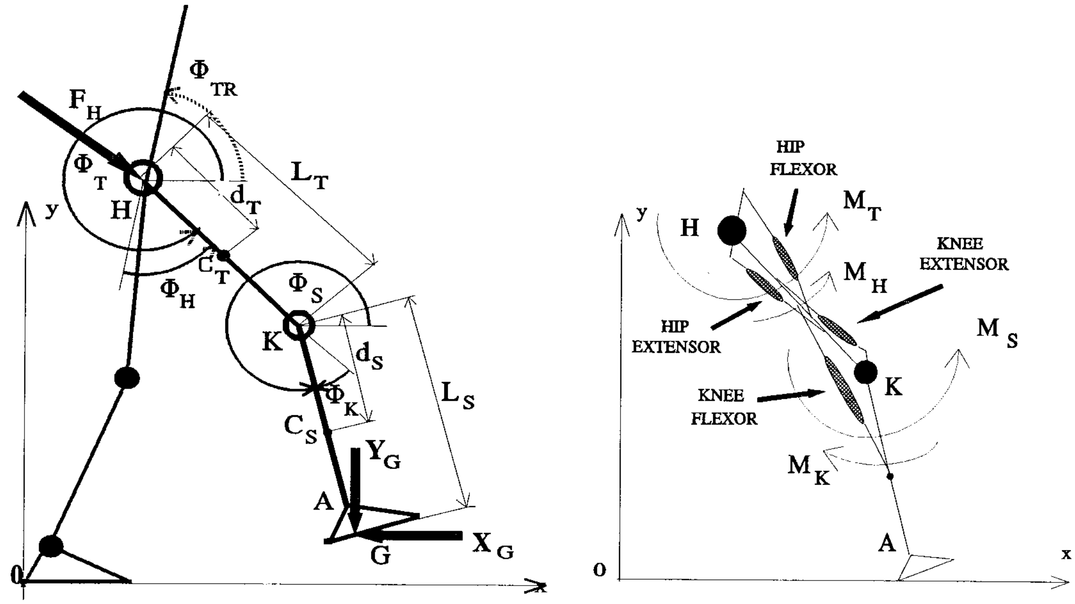

(a) (b)

Fig. 1. (a) Model of the body showing the definition of angles, segment lengths and interactive forces. (b) Model showing the muscles and torques considered.

relations at any point in the motion are solved on the basis of optimizing some criteria such as the sum of muscle forces, stress, jerk, etc. Optimal control methods that allow for the incorporation of muscle dynamics, have been used in motion synthesis [9] and optimal motion systems [15], [17], [33]. Predictions can be simulated using dynamic programming [42], [43]. Simulation of the system allows a better understanding of the details of locomotion and it can help in developing a feed-forward or a rule-based control paradigm. This study follows two previous developments: 1) a semiempiric method to determine the properties of body segments, joints and muscles of a subject with spinal cord injury (SCI) [7], [47] and 2) simulation of an externally controlled leg [38], [42], [43] or arm [50].

Here we describe an off-line analysis of excitation patterns of muscles required to produce a trajectory, taking into account the individual biomechanical parameters of the eventual user. The model considers the whole body. The model is decomposed to a body comprising one leg, trunk, head, and arms and the other leg. The simulation requires the following inputs: 1) the hip, knee and trunk angles, 2) the corresponding ground reaction forces and accelerations of the hip, and 3) body parameters, including those of the joints and muscles. The outputs of the simulation are activation patterns of the four equivalent muscles acting around the hip and knee joints. These outputs were selected for use with a simple four channel functional electrical stimulation system. An equivalent muscle is a flexor or extensor of a joint that replaces all the muscle contributing to this function [4]. Details of the optimal control algorithm are presented elsewhere [38], [50]. This information can and is intended to provide an initial stimulation pattern for paralyzed subjects to walk.

II. Methods

This study is limited to a planar model of bipedal locomotion. The model following the D'Alembert principle considers the body (arms, head, trunk and one leg) replaced by the interface force and torque acting at the hip joint, and the second leg. The leg is modeled as a planar, two segmental linkage of rigid bodies. The effects of ground reaction are included at the base. The interface to the body is included as the input for simulation. Thus, the model simulated here is reduced to a double pendulum with a moving hanging point which interfaces with the rest of the body and the ground. To make the problem tractable in a practical application, we have made some simplifying assumptions.

The double pendulum representing the leg (Fig. 1) allows knee and hip extension and flexion within physiological limits. We assume that the leg is driven by two pairs of monoarticular muscles acting around the hip and knee joints (Fig. 1). Biarticular muscles will of course add to the torques measured at each joint, but impose additional constraints that we have ignored at this stage. Estimating experimentally the relative contribution of biarticular muscles is very difficult and time-consuming [23], but will be considered in the future.

Due to various perturbations and limited strength of the hip and knee flexor and extensor muscles, the shank and thigh may not perfectly track the desired trajectory. Then, the modified shank and thigh trajectories from the prescribed one will alter the hip acceleration, velocity and position, hip and ground forces, as well as the angle of the trunk. We treated the hip acceleration, angle of the trunk versus the horizontal and ground reaction forces as inputs to the simulation, so they should remain unchanged. The solution of this problem was to assume that the subject can compensate for the changes by volitional activity of the trunk and upper extremities acting over the walker or crutches at the ground.

The model does not include active ankle and phalangeal joints, because it was assumed that a subject will wear ankle-foot orthoses (AFO) when walking to control ankle position and provide lateral stability at the ankle.

The following system of differential equations describes the dynamics:

$$\begin{aligned} & A_1\ddot{\varphi}_S + A_2\ddot{\varphi}_T\ \cos(\varphi_T-\varphi_S) + A_3\dot{\varphi}_T^2\ \sin(\varphi_T-\varphi_S) \\ &\quad - A_4\ddot{x}_H\ \sin\varphi_S - A_5(\ddot{y}_H+g)\ \cos\varphi_S \\ &\quad - X_G L_S\ \sin\varphi_S + Y_G L_S\ \cos\varphi_S = M_S \qquad (1) \\ & B_1\ddot{\varphi}_T + B_2\ddot{\varphi}_S\ \cos(\varphi_T-\varphi_S) + B_3\dot{\varphi}_S^2\ \sin(\varphi_T-\varphi_S) \\ &\quad - B_4\ddot{x}_H\ \sin\varphi_T - B_5(\ddot{y}_H+g)\ \cos\varphi_T \\ &\quad - X_G L_T\ \sin\varphi_T + Y_G L_T\ \cos\varphi_T = M_T \qquad (2) \end{aligned}$$

$$\begin{aligned} & A_1 = J_{CS} + m_S d_S^2, \quad B_1 = J_{CT} + m_S L_T^2 + m_T d_T^2 \\ & A_2 = m_S d_S L_T, \quad B_2 = A_2, \quad A_3 = -A_2, \quad B_3 = B_2 \\ & A_4 = m_S d_s, \quad B_4 = m_S L_T + m_T d_T, \\ & A_5 = -A_4, \quad B_5 = -B_4. \end{aligned}$$

The following notations are used.

S	the shank segment (including the foot);
T	the thigh segment;
CS, CT	the center of the mass of the shank and thigh segments;
H	the hip joint;
K	the knee joint;
G	the point of ground contact;
d_S, d_T	distances of the proximal joint to the centers of the masses;
L_S, L_T	lengths of the shank and thigh;
m_S, m_T	masses of the shank and thigh;
J_{CS}, J_{CT}	moments of inertia of the shank and thigh about the central axes perpendicular to xOy plane;
g	gravitational acceleration;
F_H	force acting at the hip joint;
X_G, Y_G	horizontal and vertical components of the ground reaction force;
M_S, M_T	total torques acting at the shank and thigh segments;
M_K, M_H	joint torques at the knee and hip joints;
$\ddot{x}_H, \ddot{y}_M$	horizontal and vertical components of the hip acceleration;
φ_S, φ_T	angles of the shank and thigh versus the horizontal axis (Ox);
φ_K, φ_H	angles of the knee and hip joint;
φ_{TR}	angle of the trunk versus the horizontal axis (Ox).

There are several torques contributing to the total torques acting at the links

$$\begin{aligned} & M_S = -M_K, \quad M_T = M_K + M_H \\ & M_K = M_K^f - M_K^e - M_K^r, \quad M_H = M_H^f - M_H^e - M_H^r. \end{aligned} \qquad (3)$$

Flexion of a joint is defined to be the positive direction for angular changes; hence, the flexor torque is assumed to be positive. Index f is for the equivalent flexor muscle, and index e for the equivalent extensor muscle. The contribution of passive tissue crossing the joints is included by a 'resistive' torque (index r), which will be described below in (10) and (11). The difference in the signs of the extension and flexion components of joint torques arises from the definition of the reference frame. For example, 1) hip extension is opposite to the positive direction, but 2) knee extension acts in the same direction as the positive angle in the xOy coordinate system.

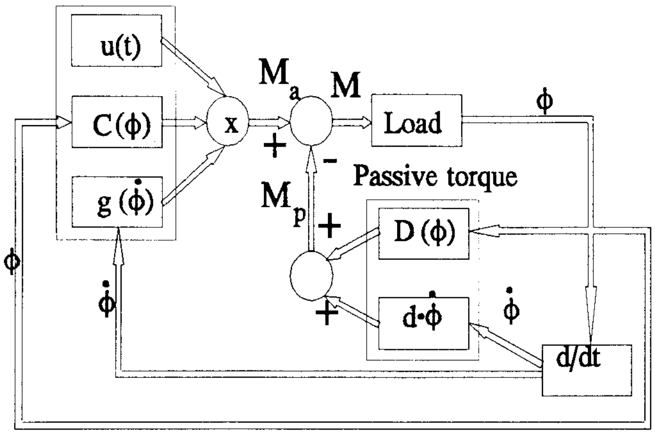

Fig. 2. Model of an equivalent muscle acting at the knee or hip joint. See text for details.

The muscle models used for simulation of equivalent flexor and extensor muscles are based on the original work of Hill [24] and Wilkie [55], which represents muscle dynamics by a contractile component and nonlinear series and parallel viscoelastic elements. The specific model used in this study is similar to the one presented recently in the literature (e.g., [51]). As shown in Fig. 2 the active joint torque depends on the product of three factors: the neural activation inputs, the length and the velocity of the muscle. The knee and hip joint angles $\varphi_K = \varphi_T - \varphi_S$ and $\varphi_H = \varphi_T - \varphi_{TR} - \pi$, and their derivatives are related to the length and the velocity of the shortening of muscles. Assuming that all of the muscles flexing the joint can be represented as a single flexor muscle, and all of the muscles extending the joint as a single extensor muscle [4], and using the modified Hill-based model of such muscles [53], [54], [57], [58] the following equations can be used (Fig. 2):

$$M_K^f = (c_{12}\varphi_K^2 + c_{11}\varphi_K + c_{10}) g_K^f(\dot{\varphi}_K) u_1 \qquad (4)$$
$$M_K^e = (c_{22}\varphi_K^2 + c_{21}\varphi_K + c_{20}) g_K^e(\dot{\varphi}_K) u_2 \qquad (5)$$
$$M_H^f = (c_{32}\varphi_H^2 + c_{31}\varphi_H + c_{30}) g_H^f(\dot{\varphi}_H) u_3 \qquad (6)$$
$$M_H^e = (c_{42}\varphi_H^2 + c_{41}\varphi_H + c_{40}) g_H^e(\dot{\varphi}_H) u_4. \qquad (7)$$

The coefficients c_{ij} $(j = 0, 1, 2; i = 1, 2, 3, 4)$ in (4)–(7) determine the best second order polynomial fit through the experimental data recorded in able-bodied or SCI subjects, and are user specific. The quadratic polynomial was selected as the simplest adequate fitting curve. The procedure for determination of the parameters is described in detail elsewhere [45], [47], [50]. Note that each of the quantities are nonnegative (i.e., if the right-hand sides of (4)–(7) go negative, the corresponding torque is set to zero).

The normalized joint torques versus joint angular velocities in (4)–(7) are determined by

$$g_K^f(\dot{\varphi}_K) = \begin{cases} c_{14}, & \dot{\varphi}_K < (1-c_{14})/c_{13} \\ 1 - c_{13}\dot{\varphi}_K, & (1-c_{14})/c_{13} \le \dot{\varphi}_K < 1/c_{13} \\ 0, & 1/c_{13} \le \dot{\varphi}_K \end{cases} \qquad (8)$$

TABLE I
BIOMECHANICAL PARAMETERS OF AN ABLE-BODIED HUMAN AND A HUMAN WITH SPINAL CORD INJURY AT T_{10} USED FOR SIMULATION

	shank - S		thigh - T	
	able-bodied subject	SCI subject	able-bodied subject	SCI subject
J_C [kgm^2]	0.23	0.21	0.19	0.18
L [m]	0.51	0.54	0.42	0.44
d [m]	0.24	0.26	0.18	0.19
m [kg]	4.5	3.2	8.1	7.2

$$g_K^e(\dot{\varphi}_K) = \begin{cases} 0, & \dot{\varphi}_K < -1/c_{23} \\ 1 + c_{23}\dot{\varphi}_K, & -1/c_{23} \le \dot{\varphi}_K < (c_{24}-1)/c_{23} \\ c_{24}, & (c_{24}-1)/c_{23} \le \dot{\varphi}_K. \end{cases} \tag{9}$$

The equations for the hip joint have the same form but the coefficients $c_{13}, c_{14}, c_{23}, c_{24}$ should be replaced with $c_{33}, c_{34}, c_{43}, c_{44}$, respectively, and index K with H. The coefficients c_{ij} $(i, 1, 2, 3, 4, j = 3, 4)$ determine the slope and saturation level of the linearized torque versus velocity of the muscle shortening. These coefficients were determined using the method described in [50].

The control inputs u_i $(i = 1, 2, 3, 4)$ are variables constrained between 0 and 1, and give the level of activation of each of the equivalent muscles, and their determination is the purpose of simulation. We intentionally used only the levels of activation to simplify the problem. A more complete model would include the activation dynamics, meaning that the activation level will be delayed after the actual electrical stimulation was applied. Then, the form of the activation would be like a low-pass filtered pulse [51]

$$M_K^r = d_{11}(\varphi_K - \varphi_{K0}) + d_{12}\dot{\varphi}_K + d_{13}e^{d_{14}\varphi_K} - d_{15}e^{d_{16}\varphi_K} \tag{10}$$

$$M_H^r = d_{31}(\varphi_H - \varphi_{H0}) + d_{32}\dot{\varphi}_H + d_{33}e^{d_{34}\varphi_H} - d_{35}e^{d_{36}\varphi_H}. \tag{11}$$

Equations (10)–(11) show the nonlinear resistive torques which depend on both the joint angle and its angular velocity. The two first terms in (10)–(11) are the contributions of passive tissues crossing the joints (dissipative properties of joints) reduced to first order functions. The other terms are the nonlinear components of the resistive torques around the terminal positions, and are modeled as double exponential curves [47]. The determination of the resistive torques is complex in humans with SCI. The parameters d_{ij} $(i = 1, 3, j = 1, 2, 3, 4, 5, 6)$ were determined from the experimental data [47]. The angles $\varphi_{K0}, \varphi_{H0}$ are the neutral positions for the knee and hip joints where the net moments are zero. Lengths and inertial parameters depicted in Fig. 1 and needed for simulation were determined using the procedure described in [47] for each individual subject (Table I).

The input file for the simulation was prepared using the processed data consisting of the angle of the trunk versus the horizontal, the hip and knee joint angles, the hip acceleration and the ground reaction forces. Data were recorded while an able-bodied subject walked on a level, powered treadmill wearing an ankle-foot orthoses for five minutes. The sensors were: four force sensing resistors built into the insole of the shoe, flexible goniometers at the leg joints, and a pendulum potentiometer at the trunk [37]. The data were captured at 100 Hz. The original kinematic and dynamic recordings were low-pass filtered at 5 Hz [52]. The components of the hip acceleration were calculated using the kinematic data. Two sets of surface electrodes recorded the EMG activities of the quadriceps and hamstring muscles. The EMG was amplified, rectified and integrated at intervals of 10 ms.

The mathematical model for simulation was derived in state space. The vector of state variables is $x = (x_1, x_2, x_3, x_4)$, where $x_1 = \varphi_S, x_2 = \dot{\varphi}_S, x_3 = \varphi_T, x_4 = \dot{\varphi}_T$. State variables in this system are constrained by the limited physiological range of motion to $0 \le \varphi_K \le \pi/2, -\pi/4 \le \varphi_H \le 3\pi/8$, and $2\pi/5 \le \varphi_{TR} \le 3\pi/5$, which implies constraints to the state variables $a \le x_1 \le b$ and $c \le x_3 \le d$, where $a = 1.15\pi, c = 0.65\pi, b = d = 1.975\pi$.

By solving the system (1)–(2) with respect to $\dot{x}_2$ and $\dot{x}_4$, we can describe the dynamics of the leg controlled by two muscle equivalents at the hip and the knee

$$\begin{aligned} \dot{x}_1 &= x_2 \\ \dot{x}_2 &= P_2 + \sum_{j=1}^{4} G_{2j}u_j \\ \dot{x}_3 &= x_4 \\ \dot{x}_4 &= P_4 + \sum_{j=1}^{4} G_{4j}u_j. \end{aligned} \tag{12}$$

The terms $P_2, P_4, G_{2j}, G_{4j}, j = 1, 2, 3, 4$ are nonlinear functions obtained as the result of a series of linear transformations of the system (1)–(11), described in [38]. In order to choose an admissible control $\boldsymbol{u} = \boldsymbol{u}(t)$ in such a way that the actual trajectory $X = X(t)$ will be as close as possible to the desired trajectory $Z = Z(t)$ and constraining the activation levels of muscles, we introduce the following *cost function*:

$$R(\boldsymbol{u}) = \int_{t_0}^{t_0+T} \{[x_1(t) - z_1(t)]^2 + [x_3(t) - z_3(t)]^2 + \lambda_1[u_1^2(t) + u_2^2(t)] + \lambda_2[u_3^2(t) + u_4^2(t)]\}\, dt. \tag{13}$$

The cost function used for the simulation is formulated in such a way that the overlap of agonist and antagonist activities is minimized, rather than the total activity of all muscles. Details of the optimization used for the simulations are in the Appendix. The algorithm was implemented using MatLab 4.2c.1—Simulink, Ver 1.3a on a PC platform.

III. RESULTS

The results show the simulation of an able-bodied human walking, as well as a subject with SCI. The gait data for both simulations (Fig. 3) were prepared using the experiments in an able-bodied subject (M.P. female, $H = 1.64$ m; $M = 56$ kg). She walked wearing ankle-foot orthoses which limited the plantar flexion to 5°, and dorsiflexion to 8°. The orthoses simulated the common pattern of walking by paraplegic subjects

TABLE II
PARAMETERS DETERMINING THE JOINT TORQUES AT THE HIP AND KNEE JOINTS FOR AN ABLE-BODIED HUMAN. ALL PARAMETERS HAVE DIMENSIONS IN INTERNATIONAL SYSTEMS

$c_{10}=61.6$	$c_{11}=1.54$	$c_{12}=-9.24$	$c_{13}=0.06$	$c_{14}=1.2$	
$c_{20}=56.45$	$c_{21}=368.67$	$c_{22}=-128.77$	$c_{23}=0.04$	$c_{24}=1.5$	
$c_{30}=206$	$c_{31}=76$	$c_{32}=-54$	$c_{33}=0.05$	$c_{34}=1.2$	
$c_{40}=158.4$	$c_{41}=114.84$	$c_{42}=-52.8$	$c_{43}=0.04$	$c_{44}=1.5$	
$d_{11}=9$	$d_{12}=0.5$	$d_{13}=0.002$	$d_{14}=5.02$	$d_{15}=50.61$	$d_{16}=-29.32$
$d_{31}=10$	$d_{32}=0.6$	$d_{33}=0.84$	$d_{34}=2.5$	$d_{35}=0.05$	$d_{36}=-14.99$

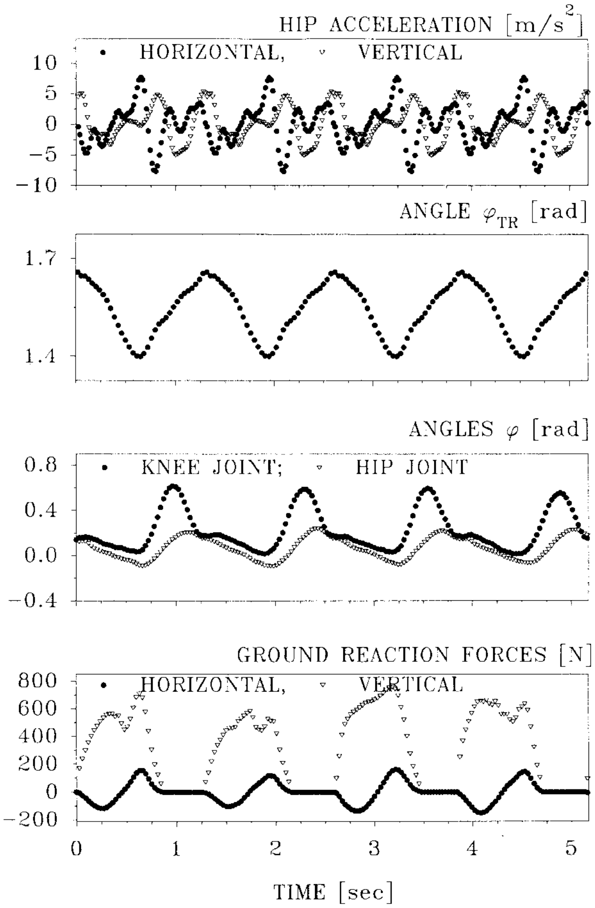

Fig. 3. Set of input data used for simulation for both, the able-boded subject and the subject with SCI. The graphs present four consecutive stride cycles starting with right heel contact. The simulation was running for many strides, but only four strides are presented to show the consistency of the model, and the variability from stride to stride.

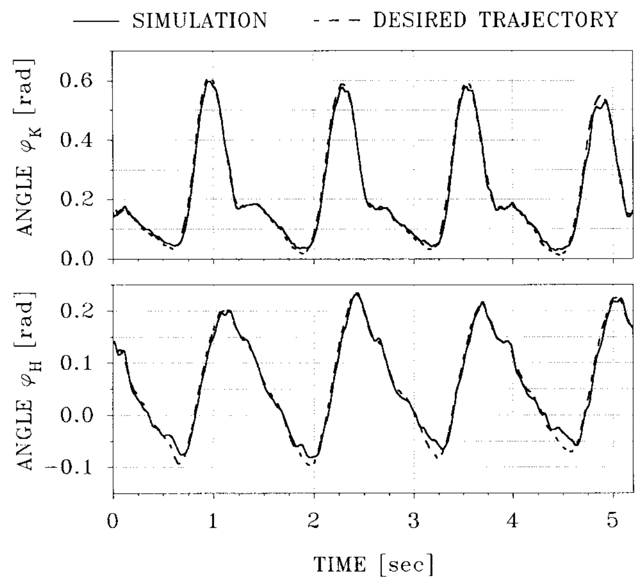

Fig. 4. Desired (input) and calculated knee and hip angles for the able-bodied subject. The error, that is the difference between the desired and calculated trajectory, is very small.

and reduced the complexity of the mathematical problem (see Section II), but did require additional forces from proximal muscles to compensate for lack of plantar flexion, for example. The stride length varied between $\Delta = 0.88$ m and $\Delta = 1.08$ m, with a stride cycle between $T = 1.24$ s and $T = 1.35$ s.

The body and muscle parameters determining the relationships between joint torque, joint angle, angular velocity and activation for the able-bodied subject are summarized in Tables I and II. The neutral angles were $\varphi_{K0} = 0.5, \varphi_{H0} = 0$.

Fig. 4 shows the recorded joint angles superimposed on the results of simulation. To measure the quality of tracking the difference between the desired angles φ_K, φ_H and the calculated values φ_K^*, φ_H^* were determined. The mean absolute errors in radians were defined

$$\overline{e}_K = \sum_{i=1}^{n} |\varphi_{K_i} - \varphi_{K_i}^*|/n, \quad \overline{e}_H = \sum_{i=1}^{n} |\varphi_{H_i} - \varphi_{H_i}^*|/n.$$

These errors have been calculated for the whole sequence of walking (230 consecutive strides) using the values sampled at every 10 ms. The magnitude of errors are $\overline{e}_K = 0.0124, \overline{e}_H = 0.083$ radians, with the standard deviations $\sigma_K = 0.0104, \sigma_H = 0.065$ radians. The maximum absolute errors were $e_{K_{\max}} = 0.06, e_{H_{\max}} = 0.13$ radians.

The joint torques (Fig. 5) were determined using the minimum cocontraction assumption (see Section II and the Appendix). The profiles of joint torques are in agreement with data in the literature for gait with a fixed ankle joint [52].

The simulation output is a set of discrete activation values for four muscle groups (Fig. 6). The agonist and antagonist muscle are deliberately presented in opposite directions to graphically display that their effect is inverted. The maximum activation is assumed to be 1, while the resting muscle is described with the activation value 0.

The simplest validation of the simulation results is to show that the actual activity of muscles (EMG) coincide with the calculated activations (Fig. 7). Note that the recorded EMG activities are from both monoarticular and biarticular muscles,

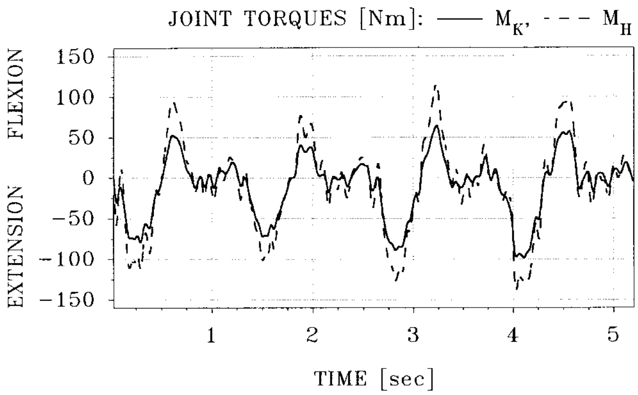

Fig. 5. Calculated joint torques at the hip and knee joints for the able-bodied subject.

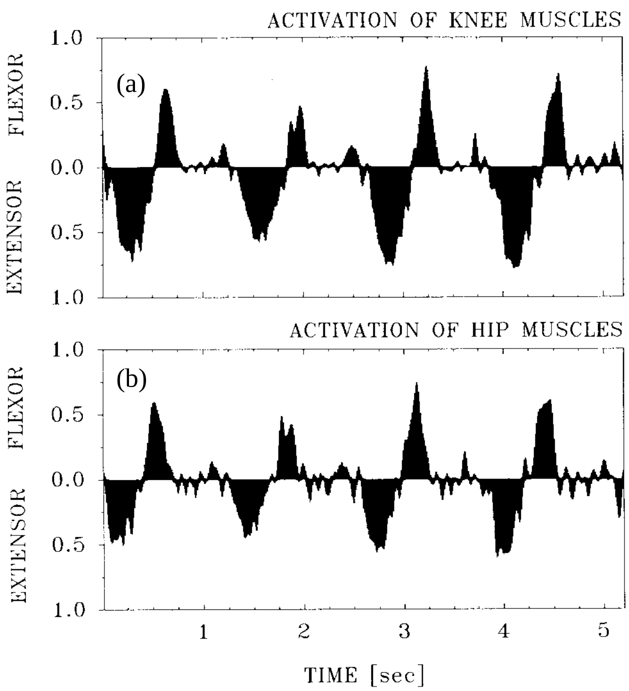

Fig. 6. Calculated levels of activation of equivalent monoarticular muscles at the hip (b) and knee joint (a) for the able-bodied subject. The top parts of both panels show the activation of flexor muscles, and the bottom parts the extensors. Note that because of the selection of the cost function cocontraction is minimized in the simulation.

and that the principle of minimum cocontraction is presumably not used for 'normal' walking. The EMG patterns are normalized to the maximum EMG activity recorded off-line when the subject was asked to generate a tetanic contraction of the given muscle group. Despite the simplifying assumptions there is a reasonable agreement between the observed EMG and predicted activation (Fig. 7). The similarity of patterns and timing validates the simulation method to some extent. The main discrepancy is the existence of cocontraction in the EMG recordings which is not seen in the simulation. This difference is due to the selected cost function (see Section IV). The minimization of cocontraction will lead to decreased periods of activating stimulated muscles, which is beneficial from the point of view of muscle fatigue, but may lead to unexpected situations because of the low stiffness of the joints.

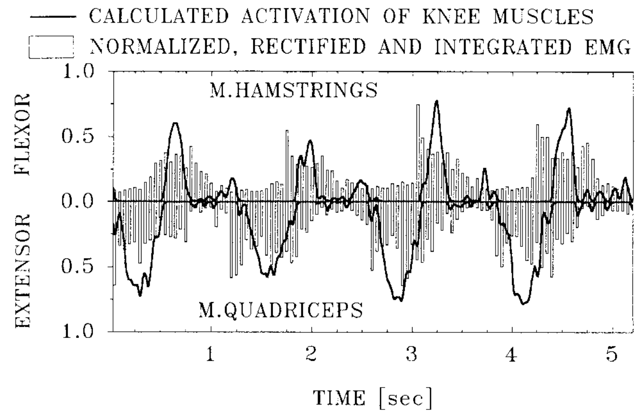

Fig. 7. Calculated activations of knee muscles and normalized, amplified, rectified, and integrated EMG recordings from the hamstrings and quadriceps muscles for the able-bodied subject.

The simulation of the gait of a subject with SCI with a lesion at T_{10} level (C.M., female, $H = 1.61$ m, $M = 52$ kg) was done by using her body and muscle parameters (Tables I and III), but the trajectory recorded from the able-bodied person walking on the powered treadmill (Fig. 3). The externally activated muscles generate forces that are smaller than the forces generated volitionally by the able-bodied subject; thus, the SCI subject was not capable of developing the joint torques that are needed to track the desired trajectory. Fig. 8 shows that due to this limitation the tracking errors were considerably more than the errors found in an able-bodied subject. The tracking errors for the subject with SCI (Fig. 8) reached $\overline{e}_K = 0.0364, \overline{e}_H = 0.1560$, the standard deviations were $\sigma_K = 0.0516, \sigma_H = 0.1611$, and the maximum errors $e_{K_{\max}} = 0.177, e_{H_{\max}} = 0.293$ radians.

The simulation shows that for a subject with SCI there is a noticeable difference between the desired hip joint force F_H and torque M_H, and calculated force and torque F_H^*, M_H^* imposed by the tracking error. The mean absolute error in the force and torque were defined as $\overline{e}_{F_H} = (1/n)\ \Sigma_{i=1}^{n}\ |F_H - F_H^*|$ and $\overline{e}_{M_n} = (1/n)\ \Sigma_{i=1}^{n}\ |M_H - M_H^*|$. Those reached $\overline{e}_{F_H} = 14.77$ N, $\overline{e}_{M_H} = 9.21$ Nm with the standard deviations $\sigma_{F_H} = 12.33, \sigma_{M_H} = 8.82$. The maximum difference between the forces is $e_{F_{\max}} = \max|F_H - F_H^*| = 51$ N, and between the joint torques $e_{M_{\max}} = \max|M_H - M_H^*| = 14.6$ Nm. Both occur at near maximum magnitudes and could be compensated by upper extremity effort to help maintain the desired trajectory.

Figs. 9 and 10 show the calculated joint torques and activation profiles for the person with SCI. Note that the activations saturate, because the muscles are not strong enough to generate adequate joint torques. We selected a trajectory for presentation where a gait pattern was achieved that was close to the desired one, even though the muscle activation saturates.

Only two examples are shown here to illustrate the algorithm. However, we tested numerous sets of input data which were collected in volunteer subjects, and the results were similar. Variation of the parameters by 10% for the able-bodied subjects produced little change in the accuracy of tracking. However, with the weaker muscles after SCI, the simulation sometimes became unstable, as is true in most

TABLE III
PARAMETERS DETERMINING THE JOINT TORQUES AT THE HIP AND KNEE JOINTS IN A HUMAN WITH SPINAL CORD INJURY AT T_{10} LEVEL. ALL PARAMETERS HAVE DIMENSIONS IN INTERNATIONAL SYSTEMS

c_{10}=28	c_{11}=0.7	c_{12}=-4.2	c_{13}=0.1	c_{14}=1.4	
c_{20}=43.2	c_{21}=282.15	c_{22}=-98.55	c_{23}=0.3	c_{24}=1.2	
c_{30}=167.37	c_{31}=61.75	c_{32}=-43.87	c_{33}=0.05	c_{34}=1.4	
c_{40}=108	c_{41}=78.3	c_{42}=-36	c_{43}=0.06	c_{44}=1.2	
d_{11}=17	d_{12}=0.6	d_{13}=0.005	d_{14}=5.048	d_{15}=98.57	d_{16}=-28.56
d_{31}=16	d_{32}=0.7	d_{33}=1.67	d_{34}=2.51	d_{35}=0.1	d_{36}=-15.04

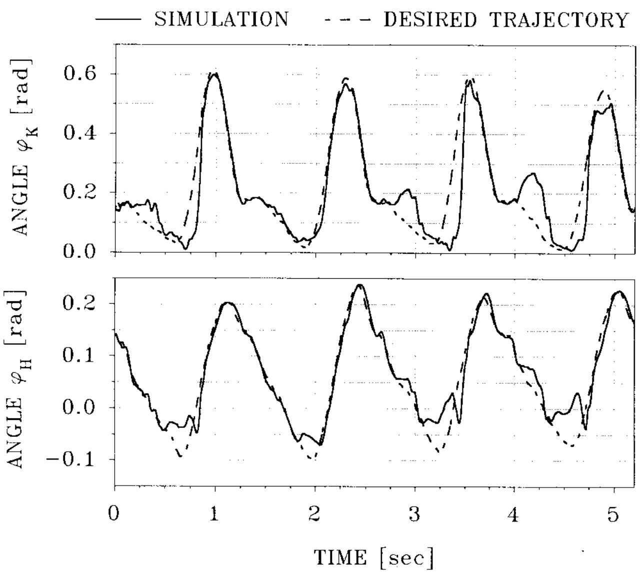

Fig. 8. Calculated trajectories of the hip and knee joints superimposed over the desired trajectory for the simulation of walking for a human with SCI. Note that the tracking error is much bigger than the one presented in Fig. 4.

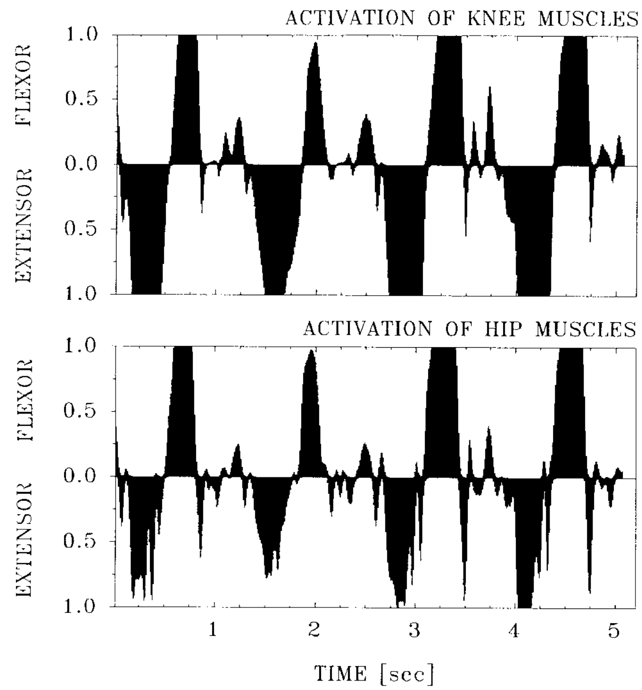

Fig. 10. Calculated activities of the equivalent hip and knee flexor and extensor muscles for a human with SCI injury. Note that there are phases of the gait cycle where the level of activity is equal to one, i.e., the muscle has to be stimulated to generate tetanic contraction, which could be very fatiguing. This is caused by the fact that the muscle forces in a human with SCI are substantially smaller than those in an able-bodied subject. The gait pattern is the same as the one used for simulating the locomotion of the able-bodied subject.

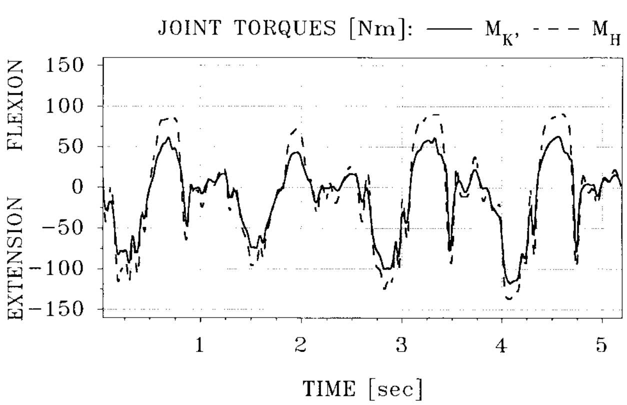

Fig. 9. Joint torques at the hip and knee joints for a human with SCI injury. The gait pattern is the same as the one used for simulating the locomotion of the able-bodied subject.

nonlinear systems. This required a sensitivity analysis of the algorithm to variation of the coefficients. There is no exact method to test the sensitivity of a nonlinear system, so the sensitivity was tested empirically by varying the parameters. The values of parameters determining the joint torques versus joint position, joint torques versus joint angular velocities, and passive joint torques were selected to ensure almost perfect tracking of the desired trajectories. The parameters were varied to determine the range in which the simulation algorithm generates the patterns of activation and ensure tracking. The maximum torques versus joint angle could be decreased by 30%, which is equivalent to a change of the coefficients $c_{ij}, i = 1,2,3,4; j = 0,1,2$ by about 20%. Increasing the maximum torques over the range of joint angles affects the simulation by reducing the levels of activation. The coefficients $c_{i4}, i = 1,2,3,4$ can be decreased up to 50% which results in increased duration of muscle activations being saturated. The coefficients $c_{i3}, i = 1,2,3,4$ affect the simulation very little and they can be reduced up to 90%. The increase of the coefficients $c_{ij}, i = 1,2,3,4, j = 3,4$ affects the simulation by decreasing the levels of activations. The coefficients determining the passive behavior of the joints $d_{ij}, i = 1,2,3,4; j = 1,2,3,4,5,6$ can be increased by

80%, and the algorithm will generate the output, while the coefficients d_{ij} can be increased by more than 80% before the simulation becomes unstable. The body parameters can be varied by 20% without causing instability of the algorithm, but the patterns of activation will change. The sensitivity of the system is highest to changes in the gait pattern. If the ground reaction forces are asynchronous with respect to the joint angles by 5%, the simulation becomes unstable. Similarly, the trunk angle must be synchronous with respect to the joint angles to within 10%.

IV. Discussion

This study starts from a model of the body determined with user-specific parameters, individualized with respect to the lengths, masses, inertia, muscle and joint properties. The trajectory used for simulation was recorded from an able-bodied subject while walking with ankles fixed using ankle-foot orthoses. The aim of the simulation was to study plausible trajectories keeping in mind the limitations imposed by the SCI (e.g., spasticity, decreased range of movements in some joints, limited strength of paralyzed, externally activated muscles). If the muscles were capable of generating the movements required and the trajectory was achieved, then the simulation provided two kinds of information: 1) timing of the onset and offset of muscle activations with respect to the various gait events; and 2) patterns of activation with respect to the maximum activation.

These results are very important for the synthesis of a rule-based control as stated in the Introduction. A rule-based control operates with a finite state representation of locomotion. This finite state representation models walking as a sequence of sensory states, and corresponding joint states, and needs only the timing of the onset and offset of muscle activations. The rules are executed as the need for a transition is recognized by changes in the sensory state; then a new motor command is issued. A sequence of state changes, turning muscles on and off, can lead to jerky movements.

A possible solution to minimize jerks when using finite state control is to introduce "soft" states into the rule-based control. These "soft" states include the continuous pattern of stimulation for individual muscles, rather then finite states that are either on or off. The "soft" states improve the control because they resolve variations in 1) the musculo-tendonous geometry from person to person, 2) the individual joint torques as a result of the disuse and atrophy of muscles, 3) the increased muscle tone which may functionally decrease the range of movements, 4) spasticity which can be very strong and interfere with the process of locomotion.

The results presented are directly applicable to the synthesis of "soft" states. There is a consistent reproducibility of the calculated activity of joint flexor and extensor muscles corresponding to the specific phases of the gait cycle. In addition, the timing is congruous with the timing of muscles in able-bodied subjects. The level of activity depends on the individual biomechanical features. In an able-bodied subject (Fig. 6) the muscles are strong enough and activations do not saturate, while in a human with SCI (Fig. 10) the maximum joint torques are not adequate and activations saturate.

In practical FES systems the activity can only be changed when a new stimulation is provided which is typically every 40 or 50 ms (25 or 20 Hz). This is considerably longer than the 10 ms interval used in the analysis, but a shorter time improves the stability of the linear programming method.

A weakness of this model is that it reduces locomotion to a planar system, and includes only four actuators per leg. The complexity of the optimization algorithm was the main reason to select this reduced model. The limitation of the analysis to only four muscle groups is still suitable for the design of an FES system which commonly only has four to six channels of stimulation for walking with ankle-foot orthoses.

The use of a multiplicative model of joint actuators is advantageous, compared to other biomechanical models that include muscles and their tendinous geometry, because the actual characteristics of the actuators can be determined experimentally. Models dealing with muscle forces require a complete knowledge about the actuators such as: muscle force versus length, muscle force versus velocity of shortening, geometry of insertion points, elasticity of tendons, etc. The muscle forces or tendon properties can not be measured directly and estimation of all the anatomical data for a given subject (e.g., point of tendon insertion, position of the center of rotation, etc.) is almost impossible. As a result these detailed models are generally not customized for individual subjects.

The validity of the model was illustrated by analyzing the actual EMG recordings and calculated patterns of activation for the able-bodied subject. The differences between the two superimposed functions are due to: 1) the calculated activations correspond to minimal cocontractions and 2) the recordings are from both biarticular and monoarticular muscles while the activations correspond only to monoarticular muscles. The mean absolute tracking errors for angles at the knee and hip joints calculated using the simulation results and desired trajectories were very small, if the muscles could generate the joint torques without being saturated. The input data varied from stride to stride, but the error remained small due to the optimization algorithm (not shown).

For the SCI subject the mean absolute tracking errors were several times larger than those calculated for the simulation of walking for the able-bodied subject. This finding was expected, because the muscle forces from the subject with SCI are smaller than the forces that an able-bodied person can develop. We analyzed components contributing to the joint torques and found that the contribution of inertial torques and torques due to the ground reactions are dominant. In fact, the ground reaction forces primarily produced the errors.

Sudden perturbations were not studied, since the model was not developed for real-time control. If perturbations can be described in terms of external torques versus position, velocity or time, they could be integrated into the mathematical model. However, a person using an FES system will be expected to balance using arm supports, so perturbations can be corrected to some extent by volitional activation of trunk and arms.

Even though the walking was rather slow, relatively large joint torques were still needed, compared to the data in the literature for able-bodied humans walking [52]. This increase results from the use of ankle-foot orthoses and the limitation to monoarticular muscles. Biarticular muscles (e.g., rectus femoris m.) are well suited for simultaneous flexion and extension of neighboring joints which occurs during several phases of the gait cycle, so integration of these muscles into the model should decrease the levels of activation. The inclusion of biarticular muscles would introduce further redundancy. This increased redundancy could be resolved by using a cost function that separates the effects of biarticular and monoarticular muscles, or by simple algebraic constraints between the torques generated by the monoarticular and biarticular muscles. However, determining appropriate constraints will require further study, and would require data that may be very difficult to measure in subjects with SCI.

The cost function used for the simulation minimizes the overlap of agonist and antagonist activity, but not the total activity of the two muscle pairs. Reducing cocontraction will reduce muscle fatigue by providing rest periods for the muscle during each step. Fatigue is often the limiting factor in application of electrical stimulation to subjects. However, the absence of cocontraction may not be completely beneficial, because in many activities, including gait, cocontraction increases stiffness and the resistance to perturbations. Including cocontraction would require a modification of the cost function (13).

Even where the simulation shows that the gait pattern is achievable, it only represents a starting point for fitting an FES controller to a person with SCI. The ground reaction forces and hip accelerations will be different in a person with SCI because of the use of upper-body support and a walker or crutches. In future work we plan to test whether this model-based approach offers practical advantages in determining initial stimulation patterns for a person with SCI, compared to the trial and error methods that are generally applied.

APPENDIX

The discrete form of (12) can be obtained if we put $h = (T - t_0)/N, t_n = t_0 + nh \wedge (n = 0, 1, \cdots, N)$ where N is a sufficiently large integer and $t_N - t_0 = T$ is the stride cycle. Further, for any $x = x(t)$ we put $x(t_n) = x_n$. Then, using the approximation $\dot{x}(t_n) = \dot{x}_n = (x_{n+1} - x_n)/h$ the motion can be described in the form

$$\begin{aligned} x_{1,n+1} &\approx x_{1,n} + hx_{2,n} \\ x_{2,n+1} &\approx x_{2,n} + h\left[P_{2,n} + \sum_{j=1}^{4} G_{2j,n}u_{j,n}\right] \\ x_{3,n+1} &\approx x_{3,n} + hx_{4,n} \\ x_{4,n+1} &\approx x_{4,n} + h\left[P_{4,n} + \sum_{j=1}^{4} G_{4j,n}u_{j,n}\right] \\ x_{i,N} &= x_{i0} \qquad (i = 1, 2, 3, 4) \end{aligned} \tag{A1}$$

and, after some manipulation and rearrangement

$$\begin{aligned} x_{1,n+2} &\approx y_{1,n} + h^2 \sum_{j=1}^{4} G_{2j,n}u_{j,n} \\ x_{3,n+2} &\approx y_{3,n} + h^2 \sum_{j=1}^{4} G_{4j,n}u_{j,n} \end{aligned} \tag{A2}$$

$$\begin{aligned} y_{1,n} &= x_{1,n} + 2hx_{2,n} + h^2P_{2,n} \\ y_{3,n} &= x_{3,n} + 2hx_{4,n} + h^2P_{4,n} \end{aligned} \tag{A3}$$

Considering the limitations in the maximum activity of muscles, the set

$$\Omega = \{(u_1, u_2, u_3, u_4)\colon 0 \le u_k \le 1 \quad (k = 1, 2, 3, 4)\}$$

will be designated as the *control region*. A control $\boldsymbol{u} = \boldsymbol{u}(t)$ will be called *admissible* if $\boldsymbol{u}(t) \in \Omega$ and it is piecewise continuous for $t_0 \le t \le t_0 + T$.

The motion of the leg is determined by the angles $\varphi_S = x_1$ and $\varphi_T = x_3$. Accordingly, we call $X(t) = (x_1(t), x_3(t)), t_0 \le t \le t_0 + T$, the trajectory. A trajectory will be called *admissible* if the state variables are within physiological constraints $a \le x_1 \le b$ and $c \le x_3 \le d$, where $a = 1.15\pi, c = 0.65\pi, b = d = 1.975\pi$. Let $Z(t) = (z_1(t), z_3(t))$, where z_1, z_3 have physiological limitations, be the desired trajectory of the functional movement. We assume that

$$x_{1,0} = z_{1,0}, \quad x_{1,N} = z_{1,N}, \quad x_{3,0} = z_{3,0}, \quad x_{3,N} = z_{3,N}. \tag{A4}$$

In order to choose an admissible control $\boldsymbol{u} = \boldsymbol{u}(t)$ in such a way that the actual trajectory $X = X(t)$ will be as close as possible to the desired trajectory $Z = Z(t)$, by constraining that the energy used is minimal we introduce the following *cost function:*

$$\begin{aligned} R(\boldsymbol{u}) = \int_{t_0}^{t_0+T} &\{[x_1(t) - z_1(t)]^2 + [x_3(t) - z_3(t)]^2 \\ &+ \lambda_1[u_1^2(t) + u_2^2(t)] + \lambda_2[u_3^2(t) + u_4^2(t)]\}.\, dt \end{aligned} \tag{A5}$$

The cost function used for the simulation imposes that the overlap of agonist and antagonist activity is minimized, but at the same time the total activity of two muscle pairs was not optimized. The values of λ_1, λ_2 can be varied between 0 and 1, and in the simulation presented they were both set at the value 1.

A discrete form of the cost function is

$$R(u) = h\left[\sum_{n=0}^{N-2} r_n(X_n, u_n) + r_{N-1}(X_{N-1}, u_{N-1})\right] \tag{A6}$$

where the terms r_n, r_{N-1} are determined by

$$\begin{aligned} r_n(X_n, u_n) = {} &\lambda_1[u_{1,n}^2 + u_{2,n}^2] + \lambda_2[u_{3,n}^2 + u_{4,n}^2] \\ &+ (x_{1,n} - z_{1,n})^2 + (x_{3,n} - z_{3,n})^2 \\ &+ \left(y_{1,n} - z_{1,n+2} + h^2 \sum_{j=1}^{4} G_{2j,n}u_{j,n}\right)^2 \\ &+ \left(y_{3,n} - z_{3,n+2} + h^2 \sum_{j=1}^{4} G_{4j,n}u_{j,n}\right)^2 \\ &(n = 0, 1, \cdots, N-2) \end{aligned} \tag{A7}$$

and

$$\begin{aligned} &r_{N-1}(X_{N-1}, u_{N-1}) \\ &\quad = \lambda_1[u_{1,N-1}^2 + u_{2,N-1}^2] \\ &\qquad + \lambda_2[u_{3,N-1}^2 + u_{4,N-1}^2]. \end{aligned} \tag{A8}$$

The optimization is now reduced to the system of (A9)

$$\frac{\partial r_n(X_n, u_n)}{\partial u_{k,n}} = 0 \qquad (k = 1, 2, 3, 4). \tag{A9}$$

Let the $\overline{u}_n = [\overline{u}_{1,n}, \overline{u}_{2,n}, \overline{u}_{3,n}, \overline{u}_{4,n}]^T$ be the solution of (A9). Then the requested optimal control is

$$\overline{u}^0_{j,n} = \begin{cases} 0, & \overline{u}_{j,n} < 0 \\ \overline{u}_{j,n}, & 0 \leq \overline{u}_{j,n} \leq 1 \\ 1, & \overline{u}_{j,n} > 1. \end{cases} \tag{A10}$$

Let the solution of the system of (A1)–(A3) be the vector $\overline{X}_n = [\overline{x}_{1,n}, \overline{x}_{2,n}, \overline{x}_{3,n}, \overline{x}_{4,n}]$. Then, put

$$\overline{x}^0_{1,n} = \begin{cases} a, & \overline{x}_{1,n} < a \\ \overline{x}_{1,n}, & a \leq \overline{x}_{1,n} \leq b \\ b, & \overline{x}_{1,n} > b \end{cases} \tag{A11}$$

$$\overline{x}^0_{3,n} = \begin{cases} c, & \overline{x}_{3,n} < c \\ \overline{x}_{3,n}, & c \leq \overline{x}_{3,n} \leq d \\ d, & \overline{x}_{3,n} > d \end{cases} \tag{A12}$$

$$\overline{x}^0_{2,n} = \overline{x}_{2,n}, \quad \overline{x}^0_{4,n} = \overline{x}_{4,n}. \tag{A13}$$

If $\{\overline{u}^0_n, \overline{X}^0_n\}$ are admissible, then they are the required optimal control and trajectory of the hip-knee system for the time interval $t_0 < t < t_0 + T$.

Further details are described in Popović *et al.* [41], [42] and Tomović *et al.* [49].

REFERENCES

[1] J. Abbas and H. J. Chizeck, "Neural network controller of functional neuromuscular stimulation systems: Computer simulation study," *IEEE Trans. Biomed. Eng.*, vol. BME-42 pp. 1117–1127, 1995.

[2] B. J. Andrews, R. W. Barnett, G. F. Phillips, C. A. Kirkwood, N. Donaldson, D. Rushton, and T. A. Perkins, "Rule-based control of a hybrid FES orthosis for assisting paraplegic locomotion," *Automed.*, vol. 11, pp. 175–199, 1989.

[3] W. W. Armstrong, "Recursive solution to the equations of motion of an n-link manipulator," in *Proc. 5th World Congr. Theory Machines and Mechanisms*, Montreal, P.Q., Canada, 1979, pp. 1343–1346.

[4] S. Bouisset, "EMG and muscle force in normal motor activities," in J. E. Desmedt, Ed., *New Developments in EMG and Clinical Neurophysiology*, vol. 1, pp. 547–583, 1973.

[5] G. S. Brindley, C. E. Polkey, and D. N. Rushton, "Electrical splinting of the knee in paraplegia," *Paraplegia*, vol. 16, pp. 428–435, 1978.

[6] E. Y. Chao and K. Rim, "Application of optimization principles in determining the applied moments in human leg joints during gait," *J. Biomech.*, vol. 6, pp. 487–510, 1973.

[7] H. J. Chizeck, R. Kobetic, E. B. Marsolais, J. J. Abbas, I. H. Donner, and E. Simon, "Control of functional neuromuscular stimulation system for standing and locomotion in paraplegics," *Proc. IEEE*, vol. 76, pp. 1155–1165, 1988.

[8] H. J. Chizeck, "Adaptive and nonlinear control methods for neuroprostheses," in *Neural Prostheses: Replacing Motor Function After Disease or Disability*, R. B. Stein, H. P. Peckham, and D. B. Popović, Eds. New York: Oxford University Press, 1992, pp. 298–327.

[9] C. K. Chow and D. H. Jacobson, "Application of optimization principles in determining the applied moments in human leg joints during gait," *J. Biomech.*, vol. 10, pp. 239–306, 1971.

[10] P. E. Crago, R. J. Nakai, and H. J. Chizeck, "Feedback regulation of hand grasp opening and contact force during stimulation of paralyzed muscles," *IEEE Trans. Biomed. Eng.*, vol. 38, pp. 17–28, 1991.

[11] R. D. Crowninshield, "Use of optimization techniques to predict muscle forces," *J. Biomech. Eng.*, vol. 100, pp. 88–92, 1978.

[12] D. T. Davy and M. L. Audu, "A dynamic optimization technique for predicting muscle forces in the swing phase of gait," *J. Biomech.*, vol. 30, pp. 187–201, 1987.

[13] H. M. Franken, P. H. Veltink, and H. B. K. Boom, "Restoring gait in paraplegics by functional electrical stimulation," *IEEE Mag. Eng. Med. Biol.*, vol. 13, pp. 564–570, 1994.

[14] H. M. Franken, P. H. Veltink, R. Tijsmans, H. Nijmeijer, and H. B. K. Boom, "Identification of quadriceps-shank dynamics using randomized interpulse interval stimulation," *IEEE Trans. Rehab. Eng.*, vol. 3, pp. 154–164, 1995.

[15] R. Happee, "Inverse dynamic optimization including muscular dynamics, a new simulation method applied to goal directed movements," *J. Biomech.*, vol. 27, pp. 953–960, 1981.

[16] D. E. Hardt, "Determining muscle forces in the leg during normal human walking: An application and evaluation of optimization model," *J. Biomech. Eng.*, vol. 100, pp. 72–78, 1978.

[17] H. Hatze, "The complete optimization of the human motion," *Math. Biosci.*, vol. 28, pp. 99–135, 1976.

[18] ——, "A complete set of control equations for the human musculo-skeletal system," *J. Biomech.*, vol. 10, pp. 799–805, 1977.

[19] ——, "A myocybernetic control model of a skeletal muscle," *Biol. Cybern.*, vol. 25, pp. 103–119, 1977.

[20] ——, "A general myocybernetic control model of skeletal muscle," *Biol. Cybern.*, vol. 28, pp. 143–157, 1978.

[21] ——, "Neuromusculoskeletal control systems modeling—A critical survey of recent developments," *IEEE Trans. Automat. Control.*, vol. AC-25, pp. 375–385, 1980.

[22] B. W. Heller, P. H. Veltink, N. J. M. Rijkhoff, W. L. C. Rutten, and B. J. Andrews, "Reconstructing muscle activation during normal walking: A comparison of symbolic and connectionist machine learning techniques," *Biol. Cybern.*, vol. 69, pp. 327–335, 1993.

[23] W. Herzog and H. E. D. J. derKeurs, "Force-length relation of *in vivo* human rectus femoris muscles," *Pfügers Arch.*, vol. 411, pp. 643–647, 1988.

[24] A. V. Hill, "The heat of shortening and the dynamic constants of muscles," *Proc. Roy. Soc.*, London, Ser. B, vol. 126, pp. 136–185, 1938.

[25] R. L. Huston, C. E. Passerello, and M. W. Harlow, "On human body dynamics," *Ann. Biomed. Eng.*, vol. 4, pp. 25–43, 1976.

[26] ——, "Dynamics of multirigid-body systems," *J. Appl. Mech.*, vol. 45, pp. 889–894, 1978.

[27] G. Khang and F. E. Zajac, "Paraplegic standing controlled by functional electrical stimulation: part I—computer model and control-system design," *IEEE Trans. Biomed. Eng.*, vol. 36, pp. 873–884, 1989.

[28] ——, "Paraplegic standing controlled by functional electrical stimulation: part II—computer simulation studies," *IEEE Trans. Biomed. Eng.*, vol. 36, pp. 885–893, 1989.

[29] C. A. Kirkwood, B. J. Andrews, and P. Mowforth, "Automatic detection of gait events: A case study using inductive learning techniques," *J. Biomed. Eng.*, vol. 11, pp. 511–516, 1989.

[30] R. Kobetic and B. Marsolais, "Synthesis of paraplegic gait with multichannel functional neuromuscular stimulation," *IEEE Trans. Rehab. Eng.*, vol. 2, pp. 66–78, 1994.

[31] S. H. Koozekanani, K. Barin, R. B. McGhee, and H. T. Chang, "A recursive free body approach to computer simulation of human postural dynamics," *IEEE Trans. Biomed. Eng.*, vol. BME-30, pp. 787–792, 1983.

[32] A. Kralj and T. Bajd, *Functional Electrical Stimulation, Standing and Walking after Spinal Cord Injury*. Boca Raton, FL: CRC Press, 1989.

[33] N. Lan and P. E. Crago, "Optimal control of antagonistic muscle stiffness during voluntary movements," *Biol. Cybern.*, vol. 71, pp. 123–135, 1994.

[34] N. Lan, H. Feng, and P. E. Crago, "Neural network generation of muscle stimulation patterns for control of arm movements," *IEEE Trans. Rehab. Eng.*, vol. 2, pp. 213–223, 1994.

[35] J. Y. S. Luh, M. W. Walker, and R. P. Paul, "On line computational scheme for mechanical manipulators," *Trans. ASME J. Dynam. Syst. Meas. Contr.*, vol. 102, pp. 69–76, 1980.

[36] E. B. Marsolais, R. Kobetic, and J. Jacobs, "Comparison of FES treatment in the stroke and spinal cord injury patient," in *Advances in External Control of Human Extremities X*, D. Popović, Ed. Nauka, Belgrade, 1990, pp. 213–218.

[37] E. Medri, D. Tepavac, B. Needham-Shropshire, and D. B. Popović, "The comprehensive system for gait analysis in handicapped persons," in *Proc. IEEE Annu. Conf. EMBS*, Baltimore, MA, 1994, pp. 1234–1235.

[38] M. N. Oğuztöreli, D. Popović, and R. B. Stein, "Optimal control for musculo-skeletal systems," *J. Automat. Contr.*, Univ. Belgrade, vol. 4, pp. 1–16, 1994.

[39] S. Onyshko and D. A. Winter, "A mathematical model for the dynamics of human locomotion," *J. Biomech.*, vol. 13, pp. 361–368, 1980.

[40] D. E. Orin, R. B. McGhee, M. Vukobratović, and G. Hartoch, "Kinematic and kinetic analysis of open-chain linkages utilizing Newton-Euler methods," *Math. Biosci.*, vol. 43, pp. 107–130, 1979.

[41] A. G. Patriarco, R. W. Mann, S. R. Simon, and J. Mansour, "An evaluation of the approaches of optimization models in prediction of muscle forces during human gait," *J. Biomech.*, vol. 14, pp. 513–525, 1981.

[42] D. Popović, M. N. Oğuztöreli, and R. B. Stein, "Optimal control for the active above-knee prosthesis," *Ann. Biomed. Eng.*, vol. 19, pp. 131–149, 1991.

[43] D. Popović, M. N. Oğuztöreli, and R. B. Stein, "Optimal control for an above-knee prosthesis with two degrees of freedom," *J. Biomech.*, vol. 29, pp. 89–98, 1995.

[44] A. Prochazka, "Comparison of natural and artificial control of movement," *IEEE Trans. Rehabil. Eng.*, vol. 1, pp. 7–17, 1993.

[45] A. Scheiner, R. B. Stein, D. Ferencz, and H. J. Chizeck, "Improved models for the lower leg in paraplegics," in *Proc. IEEE Annu. Conf. EMBS*, San Diego, CA, 1993, pp. 1151–1152.

[46] R. B. Stein, and M. N. Oğuztöreli, "Modification of muscle responses by spinal circuitry," *Neurosci.*, vol. 11, pp. 231–240, 1984.

[47] R. B. Stein, E. P. Zehr, M. K. Lebiedowska, D. B. Popović, A. Scheiner, and H. J. Chizeck, "Estimating mechanical parameters of leg segments in individuals with and without physical disabilities," *IEEE Trans. Rehab. Eng.*, vol. 4, pp. 201–212, 1996.

[48] Y. Stepanenko and M. Vukobratović, "Dynamics of articulated open-chain active mechanisms," *Math. Biosci.*, vol. 28, pp. 137–170, 1976.

[49] R. Tomović, "Skill-based expert systems," in *Intelligent Robotics Systems*, T. Tzafestas, Ed. New York: Marcel Decker, 1991, pp. 109–136.

[50] R. Tomović, D. Popović, and R. B. Stein, *Nonanalytic Methods for Motor Control*. Singapore: World Scientific, 1995.

[51] H. P. Veltink, H. J. Chizeck, P. E. Crago, and A. El-Bialy, "Nonlinear joint angle control for artificially stimulated muscle," *IEEE Trans. Biomed. Eng.*, vol. 39, pp. 368–380, 1992.

[52] D. A. Winter, *Biomechanics and Motor Control of Human Movement*, 2nd ed. New York: Wiley-Interscience, 1990.

[53] J. M. Winters, "Hill-based muscle models: A systems engineering perspective," in *Multiple Muscle Systems—Biomechanics and Movement Organization*, J. M. Winters and S. L. Y. Woo, Eds. New York: Springer-Verlag, 1990, pp. 69–73.

[54] J. M. Winters and L. Stark, "Muscle models: What is gained and what is lost by varying model complexity," *Biol. Cybern.*, vol. 55, pp. 403–420, 1987.

[55] D. R. Wilkie, "Relation between force and velocity in human muscles," *J. Physiol.*, vol. 204, pp. 443–460, 1950.

[56] G. T. Yamaguchi and F. E. Zajac, "Restoring unassisted natural gait to paraplegics via functional neuromuscular stimulation: A computer simulation study," *IEEE Trans. Biomed. Eng.*, vol. 37, pp. 886–902, 1990.

[57] G. I. Zahalak, "An overview of muscle modeling," in *Neural Prostheses: Replacing Function after Disease or Disability*, R. B. Stein, P. H. Peckham, and D. Popović, Eds. New York: Oxford University Press, 1992, pp. 17–57.

[58] F. E. Zajac, "Muscle and tendon: Properties, models, scaling and application to biomechanics and motor control," *CRC Crit. Rev. Biomed. Eng.*, vol. 17, pp. 359–411, 1989.

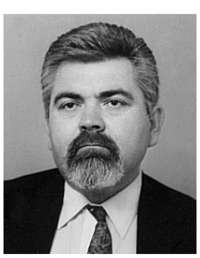

Dejan Popović was born in 1950. He received the B.Sc., M.Sc., and Ph.D. degrees from the Faculty of Electrical Engineering, Belgrade, Yugoslavia, in 1974, 1977, and 1981, respectively.

He is currently Professor of Biomedical Engineering at the Faculty of Engineering. His scientific interest is in control of movements. He is involved in the design of assistive systems for humans with physical disabilities. He contributed to many research papers in journals, books, and conference proceedings.

Dr. Popović is a member of the IEEE Engineering in Medicine and Biology Society (IEEE-EMBS) and the Yugoslav Society for ETRAN, member of the Board of directors of the IFESS, and Vice-President of the YUBEMP.

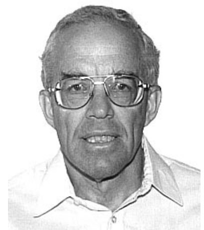

Richard B. Stein was born in New Rochelle, NY, in 1940. He received the B.S. degree in physics from Massachusetts Institute of Technology, Cambridge, and the M.A. and D.Phil. degrees in physiology from Oxford University, Oxford, U.K. He received an honorary D.Sc. degree from the University of Waterloo, Waterloo, Ont., Canada, in 1991.

Since 1968, he has been with the University of Alberta, Edmonton, Alta., Canada, and is currently Professor of Physiology and Co-Director of the Rehabilitation Neuroscience group. His research interests span a variety of areas in the control of movement such as the organization of spinal circuitry for walking, the role of reflexes in modulating behavior, properties of muscles and sensory receptors relevant to motor control and replacement of function after motor disorders such as spinal cord injury and stroke. He has authored nearly 250 scientific articles, excluding abstracts and is the founder of two Edmonton-based companies that are involved in commercialization of University-based research for persons with motor disabilities.

Dr. Stein has been President of the Canadian Physiological Society and the Canadian Association for Neuroscience. He is an Honorary member of the Deutsche EEG-Gesellschaft (German EEG Society). He received the Tesla Prize in 1998.

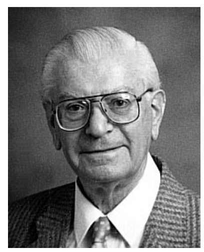

M. Namik Oğuztöreli was born January 10, 1923 in Izmir, Turkey. He received the Ph.D. degree in mathematics from the University of Istanbul, Istanbul, Turkey, in 1949.

He is a Professor Emeritus of Mathematics at the University of Alberta, Edmonton, Alta., Canada. He has authored and/or coauthored 310 papers in pure and applied mathematics, involving several interdisciplinary fields. He is also the author of a book on time-lag control systems.

Maria Lebiedowska was born in Warsaw, Poland, in 1949. She received the M.Sc. and Ph.D. degrees from Warsaw Technical University, Poland, in 1974 and 1984, respectively.

She worked for several years as a Biomedical Engineer at the Metropolitan Center of Rehabilitation, Konstancin, Poland. She organized and directed (1985–1995) the Kinesiology Laboratory at Child Health Center, Warsaw, Poland. Since 1996, she has been a Director of Motion Analysis Laboratory at Southern Illinois University, Carbondale, IL. Her research interest is in quantification of human performance and the utilization of control methods in the restoration of motor function in patients with neurological disorders.

Dr. Lebiedowska is a member of the International Society of Biomechanics, North American Society of Gait and Clinical Movement Analysis, and The Movement Disorders Society.

Slavica Jonić (S'96) was born in 1970. She received the B.Sc. degree from the Faculty of Electrical Engineering, Belgrade, Yugoslavia, in 1996. She is currently a graduate student at the Faculty of Electrical Engineering, Belgrade.

Her research interests include modeling of human motor behavior, biological signal processing, and artificial intelligence for application in the control of rehabilitation devices.

Ms. Jonić is a student member of the IEEE Engineering in Medicine and Biology Society (IEEE-EMBS).